

Nuclear size correction to the Lamb shift of one-electron atoms

Vladimir A. Yerokhin

*Center for Advanced Studies, St. Petersburg State Polytechnical University,
Polytekhnicheskaya 29, St. Petersburg 195251, Russia*

The nuclear size effect on the one-loop self energy and vacuum polarization is evaluated for the $1s$, $2s$, $3s$, $2p_{1/2}$, and $2p_{3/2}$ states of hydrogen-like ions. The calculation is performed to all orders in the binding nuclear strength parameter $Z\alpha$. Detailed comparison is made with previous all-order calculations and calculations based on the expansion in the parameter $Z\alpha$. Extrapolation of the all-order numerical results obtained towards $Z = 1$ provides results for the radiative nuclear size effect on the hydrogen Lamb shift.

PACS numbers: 31.30.jf, 12.20.Ds, 31.15.A-

Introduction

The distribution of charge of the nucleus influences the Dirac energies of atomic systems as well as the quantum electrodynamical corrections to the energy levels. This effect, termed as the nuclear size (NS) correction, is important for comparison of theoretical predictions with experimental data for the whole range of the nuclear charges Z , from hydrogen ($Z = 1$) up to uranium ($Z = 92$). The NS corrections to the one-loop self energy and vacuum polarization have been previously investigated both within the approach based on the expansion in the nuclear binding strength parameter $Z\alpha$ [1–6] (where α is the fine structure constant) and within the numerical approach that accounts the parameter $Z\alpha$ to all orders [7, 8]. In the high- Z region, the numerical all-order approach provides accurate predictions for the NS effect on the radiative corrections. For lower Z , however, the NS effect diminishes and becomes increasingly more difficult to identify in a numerical calculation. On the contrary, the $Z\alpha$ -expansion approach provides accurate predictions for the low- Z ions and only the qualitative estimates in the high- Z region. A quantitative cross-check of the two complementary approaches is not simple and has not been accomplished up to now.

The NS corrections became of particular interest recently, after the results of the muonic hydrogen Lamb-shift experiment were announced [9]. It turned out that the value for the proton charge radius r_p deduced from the muonic hydrogen differs by five standard deviations from the spectroscopic value of r_p derived from the hydrogen atom. This unexplained disagreement stimulates the scientific community to double-check all contributions originating from the nuclear charge distribution, both for the muonic and normal atoms.

The aim of the present investigation is to perform an accurate numerical all-order calculation of the NS correction to the one-loop self energy and vacuum polarization and to make a detailed comparison with the $Z\alpha$ -expansion results available.

The relativistic units ($m = \hbar = c = 1$) and the charge units $\alpha = e^2/(4\pi)$ are used in this paper.

I. NS CORRECTION TO DIRAC ENERGY

The leading-order NS correction to the energy levels of a hydrogen-like atom is defined as the difference of the corresponding eigenvalues of the Dirac equation with the point-Coulomb and the extended-nucleus potentials. The two most commonly used models of the nuclear charge distribution are the uniformly charged sphere (“sph”) and the two-parameter Fermi (“Fer”) model,

$$\rho_{\text{sph}}(r) = \rho_0 \theta(R_{\text{sph}} - r), \quad (1)$$

$$\rho_{\text{Fer}}(r) = \frac{\rho_0}{1 + \exp[(r - c)/a]}, \quad (2)$$

where $R_{\text{sph}} = \sqrt{5/3} R$ is the radius of the sphere with the root-mean-square (rms) radius R , c and a are the parameters of the Fermi distribution, and ρ_0 are the normalization factors. The parameter a of the Fermi distribution is standardly fixed by $a = 2.3/(4 \ln 3)$ fm. For a given value of the rms radius, the parameter c can be determined by the simple approximate formula

$$c^2 \approx \frac{5}{3} R^2 - \frac{7}{3} a^2 \pi^2. \quad (3)$$

In the calculations performed in this work, we will assume that the parameter c of the Fermi distribution is fixed *exactly* by the above formula.

For the uniformly charged sphere model, the Dirac equation can be solved analytically [10]. In this case, the NS correction to the Dirac energy is represented in terms of the hypergeometric function. While the exact expression is rather cumbersome, simple approximate expressions for the NS correction obtained in Ref. [10] are highly useful. For the general model of the nuclear charge distribution, the NS correction can be easily obtained by numerical solution of the Dirac equation. Numerical results are conveniently parameterized in terms of the function $G_N(Z\alpha, R)$, whose definition is inspired by the

analytic relativistic results [10],

$$\Delta E_N(ns) = \frac{(Z\alpha)^2}{n} \left(\frac{2Z\alpha R_{\text{sph}}}{n} \right)^{2\gamma} \frac{1}{10} G_N(Z\alpha, R), \quad (4)$$

$$\Delta E_N(np_{1/2}) = \frac{(Z\alpha)^4}{n} \left(\frac{2Z\alpha R_{\text{sph}}}{n} \right)^{2\gamma} \frac{n^2 - 1}{40n^2} G_N(Z\alpha, R), \quad (5)$$

where $\gamma = \sqrt{1 - (Z\alpha)^2}$ and R_{sph} is the radius of the sphere with the rms radius R . The function $G_N(Z\alpha, R)$ is a slowly varying function of $Z\alpha$ and R and its numerical values are of order of unity.

The numerical results obtained for the NS correction with the Fermi model of the nuclear charge distribution are listed in Table I. The numerical evaluation was performed by solving the Dirac equation with help of the RADIAL package [11] and, independently, by using the B-spline finite basis set method [12]. For calculations in the low- Z region, the RADIAL package was upgraded into the quadruple arithmetics (about 32 digits). The values of the rms charge radii used were taken from the compilation [13] for all ions except for uranium; the uranium rms radius was taken from Ref. [14].

II. NS CORRECTION TO SELF ENERGY

The one-loop self-energy contribution to the Lamb shift is given by a matrix element of the self-energy operator with the mass renormalization part subtracted,

$$\Delta E_{\text{SE}} = \langle a | \gamma^0 \tilde{\Sigma}(\varepsilon_a) | a \rangle, \quad (6)$$

where $\tilde{\Sigma}(\varepsilon) = \Sigma(\varepsilon) - \delta m$ and δm is the mass counterterm. The self-energy operator is [15]

$$\begin{aligned} \Sigma(\varepsilon, \mathbf{x}_1, \mathbf{x}_2) &= 2i\alpha\gamma^0 \int_{-\infty}^{\infty} d\omega D^{\mu\nu}(\omega, x_{12}) \\ &\quad \times \alpha_\mu G(\varepsilon - \omega, \mathbf{x}_1, \mathbf{x}_2) \alpha^\nu, \end{aligned} \quad (7)$$

where $D^{\mu\nu}$ is the photon propagator, G is the Dirac-Coulomb Green function, $G(\varepsilon) = (\varepsilon - H)^{-1}$, H is the Dirac-Coulomb Hamiltonian, and $\alpha^\mu = \gamma^0 \gamma^\mu$ are the Dirac matrices. The nuclear-size self-energy (NSE) correction is defined as the difference between the matrix elements (6) evaluated with the point-Coulomb potential and the potential of the extended-charge nucleus.

Numerical, all-order (in $Z\alpha$) evaluation of the one-loop self-energy correction have been extensively discussed in the literature over past decades [8, 16–20], both for the case of the point-Coulomb and extended-nucleus potentials. In the present investigation, we employ the method developed in our previous work [21] for the case of the point nucleus. This method can be immediately extended to a general (local and spherically-symmetrical) potential, provided that one can calculate the Green function

of the Dirac equation with this potential. (Beside the full Green function, the one-potential Green function is also needed in actual calculations.) In the present work, we develop an efficient scheme of computation of the Dirac Green function for a general potential, which is described in Appendix A for the full Green function and Appendix B for the one-potential Green function.

The main advantage of the method reported in Ref. [21] is a fast convergence of the partial-wave expansion of the matrix element (6). In the present work, we calculate the difference between the point-nucleus and extended-nucleus matrix elements. For this difference, the partial-wave expansion converges even faster (especially, in the low- Z region) than for the self-energy correction. Because of this, we were able to significantly improve numerical accuracy as compared to results previously reported in the literature.

Numerical results for the NSE correction to the energy shift are usually parameterized in the same way as the one-loop self-energy itself,

$$\Delta E_{\text{NSE}} = \frac{\alpha}{\pi} \frac{(Z\alpha)^4}{n^3} F_{\text{NSE}}(Z\alpha, R). \quad (8)$$

Comparison of the present results with those by Mohr and Soff [8] for the homogeneously charged sphere model is given in Table II. Numerical results obtained in the present work with the Fermi model of the nuclear charge distribution are summarized in Table III.

The leading dependence of the NSE correction on R and $Z\alpha$ can be conveniently factorized out in terms of the first-order NS contribution ΔE_N ,

$$\Delta E_{\text{NSE}}(njl) = \Delta E_N(n^{1/2}l) \frac{\alpha}{\pi} G_{\text{NSE}}(njl), \quad (9)$$

where ΔE_N is given by Eqs. (4) and (5). An important feature of this parametrization [6, 22] is that it involves the *full* NS correction, rather than only the leading term of its $Z\alpha$ expansion. With such choice of normalization, G_{NSE} is a slowly-varying function of Z and its dependence on R is more tractable. Note that for the $np_{3/2}$ reference state, Eq. (9) has $\Delta E_N(np_{1/2})$ as a prefactor, which was suggested in Ref. [6]. The $Z\alpha$ expansion of the function G_{NSE} has the form

$$\begin{aligned} G_{\text{NSE}}(ns) &= (Z\alpha) a_{10} + (Z\alpha)^2 \left[a_{\log} \ln \frac{b}{R_{\text{sph}}} \right. \\ &\quad \left. + a_{22} \ln^2(Z\alpha)^{-2} + O[\ln(Z\alpha)] \right], \end{aligned} \quad (10)$$

$$\begin{aligned} G_{\text{NSE}}(np_j) &= a_{01} \ln(Z\alpha)^{-2} + a_{00} \\ &\quad + (Z\alpha) a_{10} + (Z\alpha)^2 \left[a_{\log} \delta_{j,1/2} \ln \frac{b}{R_{\text{sph}}} \right. \\ &\quad \left. + a_{21} \delta_{j,1/2} \ln(Z\alpha)^{-2} + O(1) \right], \end{aligned} \quad (11)$$

where $b = \exp[1/(2\gamma) - C - 5/6]$, $\gamma = \sqrt{1 - (Z\alpha)^2}$, and C is the Euler constant. Known results for the coefficients of the expansion are listed in Table IV. We note

that the logarithmic a_{22} and a_{21} terms have not yet appeared in the literature. It was, however, pointed out by Pachucki [23] that such terms are present and that the coefficients for the leading logarithms ($\ln^2(Z\alpha)$ for ns states and $\ln(Z\alpha)$ for $np_{1/2}$ states) are the same as for the self-energy correction to the hyperfine splitting. Values of $a_{00}(np_{1/2})$ for $n > 2$ can be found in Ref. [5].

Comparison of the present numerical data for the function G_{NSE} with the $Z\alpha$ -expansion results is given in three upper graphs of Fig. 1. Note that for ns states, the ratio $G_{\text{NSE}}(Z\alpha)/(Z\alpha)$ is plotted. The lower graphs in Fig. 1 depict the higher-order remainder (i.e., the contribution beyond the known terms of the $Z\alpha$ expansion). For ns states, the remainder does not approach a finite limit as $Z \rightarrow 0$ because it contains $\ln(Z\alpha)$, as can be seen from Eqs. (10) and (11).

In Fig. 2, the dependence of G_{NSE} on the rms nuclear charge radius R is studied, with the nuclear charge number fixed by $Z = 92$. We find that the R dependence of our numerical data can be well approximated by a three-parameter fit that includes $\ln R$, as suggested by the $Z\alpha$ expansion. More specifically, the following fitting functions approximate the numerical data for $Z = 92$ in the region $R = 3\text{--}12$ fm with the relative accuracy of better than 2×10^{-4} (with R expressed in fermi units),

$$G_{\text{NSE}}(R; 1s) = -11.8768 + 1.2083 \ln R + 0.0191 R, \quad (12)$$

$$G_{\text{NSE}}(R; 2s) = -12.2394 + 1.2124 \ln R + 0.0220 R, \quad (13)$$

$$G_{\text{NSE}}(R; 3s) = -11.9131 + 1.2143 \ln R + 0.0218 R, \quad (14)$$

$$G_{\text{NSE}}(R; 2p_{1/2}) = -9.4115 + 1.1759 \ln R + 0.0098 R, \quad (15)$$

$$G_{\text{NSE}}(R; 2p_{3/2}) = -1.0145 + 0.0019 \ln R + 0.0033 R. \quad (16)$$

III. NS CORRECTION TO VACUUM POLARIZATION

The one-loop vacuum-polarization correction to the energy levels is usually represented as a sum of two parts, the Uehling and the Wichmann-Kroll ones [15]. The Uehling part of the vacuum polarization is given by the expectation value of the potential

$$U_{\text{Ueh}}(r) = -\frac{2\alpha^2 Z}{3mr} \int_0^\infty dr' r' \rho(r') \times [K_0(2m|r - r'|) - K_0(2m|r + r'|)], \quad (17)$$

where

$$K_0(x) = \int_1^\infty dt e^{-xt} \left(\frac{1}{t^3} + \frac{1}{2t^5} \right) \sqrt{t^2 - 1}, \quad (18)$$

and the nuclear-charge density ρ is normalized by the condition $\int dr \rho(r) = 1$. The energy shift due to the

Wichmann-Kroll part of the vacuum polarization can be written as [7, 24]

$$\Delta E_{\text{WK}} = \frac{2\alpha}{\pi} \text{Re} \sum_{\kappa} |\kappa| \int_0^\infty d\omega \int_0^\infty r^2 dr (g_a^2 + f_a^2) \times \int_r^\infty dr' r' \left(1 - \frac{r'}{r} \right) \text{Tr} G_{\kappa}^{(2+)}(i\omega, r', r'), \quad (19)$$

where g_a and f_a are the upper and the lower radial components of the reference-state wave function, $G_{\kappa}^{(2+)}$ is the radial Dirac Green function that contains two and more interactions with the binding field,

$$G_{\kappa}^{(2+)}(\omega, x, y) = \int_0^\infty dz z^2 G_{\kappa}^{(0)}(\omega, x, z) V(z) \times [G_{\kappa}(\omega, z, y) - G_{\kappa}^{(0)}(\omega, z, y)], \quad (20)$$

G_{κ} is the radial part of the full Dirac Green function, $G_{\kappa}^{(0)}$ is the free Dirac Green function, and $V(z)$ is the binding potential. We note that Eq. (19) is valid both for the point-nucleus and the extended-nucleus binding potentials.

Calculations of the Wichmann-Kroll part of the one-loop vacuum polarization were extensively discussed in the literature over past decades [7, 24–26]. In the present work, we perform calculations of the vacuum polarization, evaluating the integrations and the summation over κ in the order specified by Eqs. (19) and (20). Comparison of the numerical results obtained in this work for the Wichmann-Kroll correction with those reported in previous calculations [15, 25] is presented in Table V.

The nuclear-size vacuum-polarization (NVP) correction is defined as the difference between the one-loop vacuum-polarization corrections evaluated with the point-Coulomb potential and the potential of the extended-charge nucleus. The NVP correction can be parameterized in the same way as the one-loop radiative corrections,

$$\Delta E_{\text{NVP}} = \frac{\alpha}{\pi} \frac{(Z\alpha)^4}{n^3} F_{\text{NVP}}(Z\alpha, R). \quad (21)$$

The results of our numerical evaluation of the NVP correction for the $1s$, $2s$, $3s$, $2p_{1/2}$, and $2p_{3/2}$ states of H-like ions are presented in Table VI. The calculation is performed for the Fermi model of the nuclear charge distribution. It is interesting to note that for the $2p_{3/2}$ state and high nuclear charges, the correction coming from the Wichmann-Kroll part of the vacuum polarization dominates over the Uehling part.

The leading dependence of the NVP correction on R and $Z\alpha$ can be conveniently factorized out in terms of the first-order NS contribution $\Delta E_{\text{N}} [6, 22]$,

$$\Delta E_{\text{NVP}}(njl) = \Delta E_{\text{N}}(n1/2l) \frac{\alpha}{\pi} G_{\text{NVP}}(njl). \quad (22)$$

Note that similarly to the NSE correction, for the $np_{3/2}$ reference state, Eq. (22) has the first-order NS correction for the $np_{1/2}$ state as a prefactor.

The $Z\alpha$ expansion of the function G_{NVP} is given by

$$G_{\text{NVP}}(ns) = (Z\alpha) a_{10} + (Z\alpha)^2 \left[\frac{2}{3\gamma} \ln^2 \frac{b}{R_{\text{sph}}} + a_{21} \ln(Z\alpha)^{-2} + f(Z\alpha, R_{\text{sph}}) + O(1) \right], \quad (23)$$

$$G_{\text{NVP}}(np_j) = a_{00} + (Z\alpha) a_{10} + (Z\alpha)^2 \left[\frac{2}{3\gamma} \delta_{j,1/2} \ln^2 \frac{b}{R_{\text{sph}}} + \delta_{j,1/2} f(Z\alpha, R_{\text{sph}}) + O(1) \right], \quad (24)$$

where $b = \exp[1/(2\gamma) - C - 5/6]$, $\gamma = \sqrt{1 - (Z\alpha)^2}$, and C is the Euler constant. The leading term of the expansion for the s states was calculated long ago [1, 2]. All other coefficients except a_{21} were derived in Refs. [4, 6]. The logarithmic a_{21} term was pointed out by Pachucki [23]; the value of the coefficient is the same as for the vacuum-polarization correction to the hyperfine splitting. The results for the expansion coefficients are

$$a_{00}(np_{1/2}) = a_{00}(np_{3/2}) = -8/45, \quad (25)$$

$$a_{10}(ns) = 3\pi/4, \quad a_{10}(np_{1/2}) = 23\pi/72, \quad a_{10}(np_{3/2}) = 5\pi/72, \quad (26)$$

$$a_{21}(ns) = 4/15, \quad (27)$$

and [6]

$$f(Z\alpha, R_{\text{sph}}) = \frac{1}{3(Z\alpha)^2} \left[-2 \ln R_{\text{sph}} - \frac{5}{3} + \pi \tan(\pi\gamma) + \frac{2}{3 + 2\gamma} + 2\psi(-1 - 2\gamma) - \frac{\pi^{3/2}(3 + 2\gamma)\Gamma(\gamma + 1)}{40 \sin(2\pi\gamma)(\gamma - 1)\Gamma(-1 - 2\gamma)\Gamma(\gamma + 3/2)} \times (2R_{\text{sph}})^{2(1-\gamma)} \right]. \quad (28)$$

The function $f(Z\alpha, R_{\text{sph}})$ has a finite limit as $Z\alpha \rightarrow 0$, which is

$$f(0, R_{\text{sph}}) = \frac{1}{3} \ln^2 R_{\text{sph}} + \left(-\frac{4}{5} + \frac{2}{3} C \right) \ln R_{\text{sph}} + \frac{1}{3} \left(\frac{833}{255} - \frac{12}{5} C + C^2 - \frac{\pi^2}{12} \right). \quad (29)$$

In Fig. 3, we compare the present numerical data for the function G_{NVP} with the $Z\alpha$ -expansion results summarized above. We observe good agreement in all cases; the higher-order remainder function exhibits a nearly linear dependence on the nuclear charge number.

In Fig. 4, we study the dependence of the function G_{NVP} on the rms nuclear charge radius R , with the nuclear charge number fixed by $Z = 92$. Similarly to the

NSE correction, we find that the R dependence of our numerical data can be well approximated by a three-parameter fit, whose form is suggested by the $Z\alpha$ expansion. More specifically, the following fitting functions approximate the numerical data for $Z = 92$ in the region $R = 3\text{--}12$ fm with the relative accuracy of better than 2×10^{-4} (with R expressed in fermi units),

$$G_{\text{NVP}}(R; 1s) = 15.3607 + 0.3459 \ln^2 R - 4.4325 \ln R, \quad (30)$$

$$G_{\text{NVP}}(R; 2s) = 15.5292 + 0.3397 \ln^2 R - 4.4307 \ln R, \quad (31)$$

$$G_{\text{NVP}}(R; 3s) = 15.4820 + 0.3396 \ln^2 R - 4.4321 \ln R, \quad (32)$$

$$G_{\text{NVP}}(R; 2p_{1/2}) = 14.3668 + 0.3673 \ln^2 R - 4.4346 \ln R, \quad (33)$$

$$G_{\text{NVP}}(R; 2p_{3/2}) = -0.02474 - 0.000134 R + 0.000001 R^2. \quad (34)$$

IV. RESULTS FOR HYDROGEN

In this section, we obtain all-order (in $Z\alpha$) results for the radiative nuclear size effect to the ground-state Lamb shift in hydrogen. This task is complicated by the fact that we are not able to perform calculations of the self-energy and Wichmann-Kroll parts of the nuclear size effect directly for $Z = 1$. In the absence of a direct calculation, we perform extrapolation of the numerical data obtained for higher values of Z to $Z = 1$.

We start with the self energy. The data for the function $G_{\text{NSE}}(Z, R)$ plotted in Fig. 1 is not well suited for extrapolation since individual points correspond to different values of the rms radius. Because of this, we repeat our calculations for different nuclear charges and the rms radius fixed by $R = r_p$, where $r_p = 0.8768(69)$ fm is the CODATA value of the proton charge radius [27]. We also account for the fact that the Fermi model of the nuclear charge distribution is not completely adequate for small rms radii; the Gaussian model is employed instead, with $\rho(r) = \rho_0 \exp(-\Lambda r^2)$. The extrapolation is performed for the higher-order remainder function,

$$\mathcal{G}_{\text{NSE}}^{\text{h.o.}} = [G_{\text{NSE}}(\text{num}) - G_{\text{NSE}}(\text{ana})]/(Z\alpha), \quad (35)$$

where $G_{\text{NSE}}(\text{num})$ and $G_{\text{NSE}}(\text{ana})$ denote the numerical and analytical [Eq. (10)] values of the G_{NSE} function. In our extrapolation, we used 20 points with the nuclear charges in the interval $Z = 5\text{--}30$ and the same extrapolation procedure as in Ref. [28]. Our result for hydrogen is $\mathcal{G}_{\text{NSE}}^{\text{h.o.}}(Z = 1) = 0.075(25)$.

The Uehling part of the NVP correction is calculated directly, with the result (for the Gaussian model) $G_{\text{NVP, Ue}}(Z = 1) = 2.5835\alpha$. The Wichmann-Kroll part is a small correction for hydrogen, its leading contribution to G_{NVP} being a constant term of order $(Z\alpha)^2$. Similarly to the NSE correction, we obtain

the result for hydrogen by extrapolation. The data to be extrapolated is obtained by repeating our calculations for $Z = 20 - 75$, with the rms radius fixed by $R = r_p$ and the nuclear charge distribution given by the Gaussian model. The extrapolation is performed for the ratio $G_{\text{NVP,WK}}/(Z\alpha)^2$. The result for hydrogen is $G_{\text{NVP,WK}}(Z=1) = -9.8(9)\alpha^2$.

Summarising our calculations of the radiative nuclear size effect to the $1s$ Lamb shift in hydrogen, we express the results in the same form as in Ref. [27],

$$\Delta E_{\text{NSE}} = \alpha^2 Z \mathcal{E}_N [-3.1294(80)], \quad (36)$$

$$\Delta E_{\text{NVP}} = \alpha^2 Z \mathcal{E}_N [0.8228 - 0.0228(23)], \quad (37)$$

where $\mathcal{E}_N = 2/3 (Z\alpha)^4 R^2$ and the first and the second terms in the brackets in Eq. (37) correspond to the Uehling and Wichmann-Kroll parts. In order to estimate the model dependence of our results, we evaluated the Uehling part also within the exponential model, with $\rho(r) = \rho_0 \exp(-\Lambda r)$, and found a 0.2% deviation from the Gaussian result.

The numerical constant terms in Eqs. (36) and (37) can be compared with the $Z\alpha$ -expansion results. For the self-energy, the leading-order term of the $Z\alpha$ expansion is $4 \ln 2 - 23/4 = -2.977$, whereas all terms in Eq. (10) yield the coefficient of -3.153 . For the vacuum polarization, the leading-order term is $3/4$, whereas all terms in Eq. (23) yield 0.827 . We conclude that the higher-order corrections increase the leading-order result for the radiative nuclear size effect in hydrogen by 4.4%.

Conclusion

In the present investigation, we evaluate the nuclear size correction to the Lamb shift of the $1s$, $2s$, $3s$, $2p_{1/2}$, and $2p_{3/2}$ states of hydrogen-like atoms. The treatment is complete at the one-loop level, i.e., it includes the leading-order effect as well as the one-loop radiative corrections. The total nuclear size correction to the energy level is represented, for the ns and $np_{1/2}$ states, as

$$\Delta E_{\text{NS}} = \Delta E_N \left[1 + \frac{\alpha}{\pi} (G_{\text{NSE}} + G_{\text{NVP}}) \right], \quad (38)$$

and, for the $np_{3/2}$ states, as

$$\begin{aligned} \Delta E_{\text{NS}}(np_{3/2}) &= \Delta E_N(np_{3/2}) \\ &+ \Delta E_N(np_{1/2}) \frac{\alpha}{\pi} (G_{\text{NSE}} + G_{\text{NVP}}), \end{aligned} \quad (39)$$

where ΔE_N is the nuclear size correction to the Dirac energy. The all-order numerical values obtained for the self-energy and vacuum-polarization functions G_{NSE} and G_{NVP} were compared with results of the $Z\alpha$ -expansion calculations. Inclusion of the logarithmic term of the relative order $(Z\alpha)^2 \ln^2(Z\alpha)^{-2}$ for ns states was necessary

in order to achieve agreement between different calculations. Extrapolation of the all-order data obtained for hydrogen-like ions to $Z = 1$ provides an all-order result for the radiative nuclear size effect on the ground-state Lamb shift in hydrogen. The higher-order corrections are shown to increase the leading-order result by 4.4%.

Acknowledgments

I wish to thank Krzysztof Pachucki for valuable comments and advices. Computations reported in this work were performed on the computer cluster of St. Petersburg State Polytechnical University.

Appendix A: Dirac Green function for a general potential

In this section we construct the Green function of the Dirac equation with the potential $V(r)$ of a general form. We assume that the potential $V(r)$ differs from the Coulomb one within a finite (inner) region only, i.e., there is r_0 such that, for $r > r_0$, $V(r) = -Z\alpha/r$, with $Z \geq 0$. For our purposes, it is sufficient to consider the potential to be regular at the origin, i.e., $rV(r) \rightarrow 0$ as $r \rightarrow 0$. In the inner region $r < r_0$, the combination $rV(r)$ is assumed to be well represented by a piecewise cubic polynomial calculated on a sufficiently dense grid.

The radial Dirac Green function $G_\kappa(E, r_1, r_2)$ is expressed in terms of the two-component solutions of the radial Dirac equation regular at the origin (ϕ_κ^0) and the infinity (ϕ_κ^∞) as follows

$$\begin{aligned} G_\kappa(E, r_1, r_2) &= -\phi_\kappa^\infty(E, r_1) \phi_\kappa^{0T}(E, r_2) \theta(r_1 - r_2) \\ &- \phi_\kappa^0(E, r_1) \phi_\kappa^{\infty T}(E, r_2) \theta(r_2 - r_1). \end{aligned} \quad (\text{A1})$$

The solutions are normalized by the condition that their Wronskian is unity (everywhere except for the bound-state energies),

$$\phi_\kappa^{0T}(E, r) \begin{pmatrix} 0 & -1 \\ 1 & 0 \end{pmatrix} \phi_\kappa^\infty(E, r) = 1. \quad (\text{A2})$$

In the present work, we obtain the radial solutions in the inner region $r < r_0$ by a numerical solution of the Dirac equation on a grid, whereas in the outer region $r > r_0$, we express them as a combination of the radial solutions of the Dirac-Coulomb problem. The regular and irregular solutions of the Dirac equation with the point-nucleus Coulomb potential will be denoted by ψ_κ^0 and ψ_κ^∞ , respectively. They are known analytically in terms of the Whittaker functions, see e.g., Ref. [15]. (Note the sign difference of the present definition of the Green function as compared to that of Ref. [15].) In this work, the Dirac-Coulomb solutions ψ_κ^0 and ψ_κ^∞ are evaluated by a generalization of the procedure described in Ref. [20].

TABLE I: Nuclear-size correction to the Dirac energies of H-like ions, in terms of the function $G_N(Z\alpha, R)$ defined by Eq. (4). Fermi model of the nuclear charge distribution is used.

Z	R [fm]	$1s$	$2s$	$3s$	$2p_{1/2}$
5	2.4059	1.000 46	1.000 71	1.000 23	1.001 73
8	2.7013	1.003 91	1.004 55	1.003 33	1.006 89
10	3.0053	1.006 57	1.007 58	1.005 67	1.011 17
15	3.1888	1.015 66	1.017 93	1.013 60	1.025 66
20	3.4764	1.028 67	1.032 74	1.024 91	1.046 42
26	3.7371	1.049 77	1.056 75	1.043 18	1.080 18
30	3.9286	1.067 32	1.076 73	1.058 28	1.108 52
40	4.2696	1.124 66	1.142 02	1.106 96	1.202 64
50	4.6543	1.203 59	1.232 01	1.172 31	1.337 09
60	4.9118	1.308 62	1.351 81	1.256 25	1.524 64
70	5.3115	1.445 02	1.507 15	1.359 74	1.784 78
82	5.5010	1.662 15	1.752 74	1.511 54	2.236 31
92	5.8569	1.896 75	2.013 31	1.655 09	2.785 73
100	5.8570	2.128 53	2.263 06	1.774 54	3.393 88

TABLE II: Different calculations of the nuclear-size self-energy correction to the energy levels of H-like ions, in terms of the function $F_{\text{NSE}}(Z\alpha, R)$ defined by Eq. (8), for the homogeneously charged sphere model.

Z	R [fm]	$1s$	$2s$	$2p_{1/2}$	Ref.
26	3.730	−0.000 172 122(4)	−0.000 173 29(1)	0.000 000 972(2)	[8]
		−0.000 172(1)	−0.000 18(1)	−0.000 00(1)	
54	4.826	−0.001 274 870(2)	−0.001 461 69(1)	−0.000 020 391(2)	[8]
		−0.001 275(1)	−0.001 462(1)	−0.000 021(1)	
92	5.863	−0.018 491 8(8)	−0.029 089 3(9)	−0.002 482 76(8)	[8]
		−0.018 492(1)	−0.029 090(2)	−0.002 483(1)	

The general calculational scheme is as follows. For a given energy argument E , we calculate and store the solutions ψ_κ^0 and ψ_κ^∞ on a radial grid $\{r_i\}_{i=1}^N$ and then obtain the radial Green function for arbitrary radial arguments by interpolation. Large number of the mesh points ($N \sim 10^4$) and a careful choice of the grid allow us to minimize losses of accuracy due to interpolation. In order to avoid numerical overflow (underflow) when storing the regular and irregular solutions for large imaginary energies E and large κ , all manipulations are performed with the “normalized” solutions in which the approximate large- r and small- r behaviour is pulled out,

$$\tilde{\phi}_\kappa^0(E, r) = r^{-|\kappa|} e^{-cr} \phi_\kappa^0(E, r), \quad (\text{A3})$$

$$\tilde{\phi}_\kappa^\infty(E, r) = r^{|\kappa|} e^{cr} \phi_\kappa^\infty(E, r), \quad (\text{A4})$$

where $c = \sqrt{1 - E^2}$. Advantages of the normalized solutions are, first, that they are more suitable for interpolation than the original solutions and, more importantly, that they can be stored and manipulated within the standard double precision arithmetics (in the range of κ ’s relevant for the present investigation, up to $|\kappa| \sim 30$).

In the inner region $r < r_0$, we calculate the regular solution ϕ_κ^0 (or, rather, $\tilde{\phi}_\kappa^0$) by solving the radial Dirac equation on a grid as described in the following, starting from $r = 0$ and up to $r = r_0$. For $r > r_0$, the potential is the Coulomb one and the regular solution ϕ_κ^0 is a linear

combination of the regular and irregular Dirac-Coulomb solutions,

$$\phi_\kappa^0(E, r) = a \psi_\kappa^0(E, r) + b \psi_\kappa^\infty(E, r), \quad r \geq r_0. \quad (\text{A5})$$

The coefficients a and b are defined by the condition that the two components of ϕ_κ^0 are continuous at $r = r_0$. So, we determine the coefficients a and b by matching the numerical and the analytical solutions at $r = r_0$ and employ the analytical Dirac-Coulomb functions for calculations for $r > r_0$.

The irregular solution ϕ_κ^∞ in the outer region is just the Dirac Coulomb function,

$$\phi_\kappa^\infty(E, r) = \psi_\kappa^\infty(E, r), \quad r \geq r_0. \quad (\text{A6})$$

So, we use the analytical representation for $r \geq r_0$. For smaller r , the irregular solution is calculated by solving the Dirac equation on a grid, downward from $r = r_0$ towards $r = 0$. The normalization of the numerical solution is fixed by requiring continuity at the point $r = r_0$.

We now turn to the problem of solving the Dirac equation with the potential $V(r)$ on a grid. In this work, we employ the power series solution method, previously applied to the Dirac equation by Salvat et al. [11]. For completeness, we give here the description of the method. First, let us solve the equation on the interval $[r_a, r_b]$ with given boundary conditions at $r = r_a$. The situation

TABLE III: Nuclear-size self-energy correction to the energy levels of H-like ions, in terms of the function $F_{\text{NSE}}(Z\alpha, R)$ defined by Eq. (8). Fermi model of the nuclear charge distribution is used. The nuclear charge rms radii used are listed in Table I.

Z	$1s$	$2s$	$3s$	$2p_{1/2}$	$2p_{3/2}$
5	-0.000 009 962(6)	-0.000 009 81(2)			
8	-0.000 020 969(2)	-0.000 020 53(1)		0.000 000 107(8)	
10	-0.000 033 242(2)	-0.000 032 54(1)	-0.000 032 12(3)	0.000 000 201(4)	0.000 000 170(2)
15	-0.000 060 128(2)	-0.000 059 10(1)	-0.000 058 21(4)	0.000 000 412(2)	0.000 000 345(2)
20	-0.000 102 940(2)	-0.000 102 06(2)	-0.000 100 38(2)	0.000 000 699(2)	0.000 000 587(2)
26	-0.000 172 537(2)	-0.000 173 71(3)	-0.000 170 72(3)	0.000 000 976(2)	0.000 000 852(2)
30	-0.000 238 936(2)	-0.000 243 68(3)	-0.000 239 45(3)	0.000 001 021(2)	0.000 000 969(2)
40	-0.000 481 097(2)	-0.000 511 07(2)	-0.000 502 4(1)	-0.000 000 726(2)	0.000 000 396(2)
50	-0.000 960 607(2)	-0.001 075 22(2)	-0.001 057 8(1)	-0.000 010 544(2)	-0.000 003 299(2)
60	-0.001 830 75(1)	-0.002 183 28(2)	-0.002 150 3(4)	-0.000 046 025(4)	-0.000 014 862(2)
70	-0.003 730 19(4)	-0.004 791 85(6)	-0.004 722 0(2)	-0.000 170 450(6)	-0.000 047 078(2)
82	-0.008 404 0(2)	-0.011 977 2(2)	-0.011 796 6(4)	-0.000 703 91(2)	-0.000 140 462(2)
92	-0.018 426 6(7)	-0.028 986 6(8)	-0.028 474 0(6)	-0.002 473 96(6)	-0.000 337 183(2)
100	-0.034 060(2)	-0.058 444(3)	-0.057 172(1)	-0.006 696 3(4)	-0.000 602 404(2)

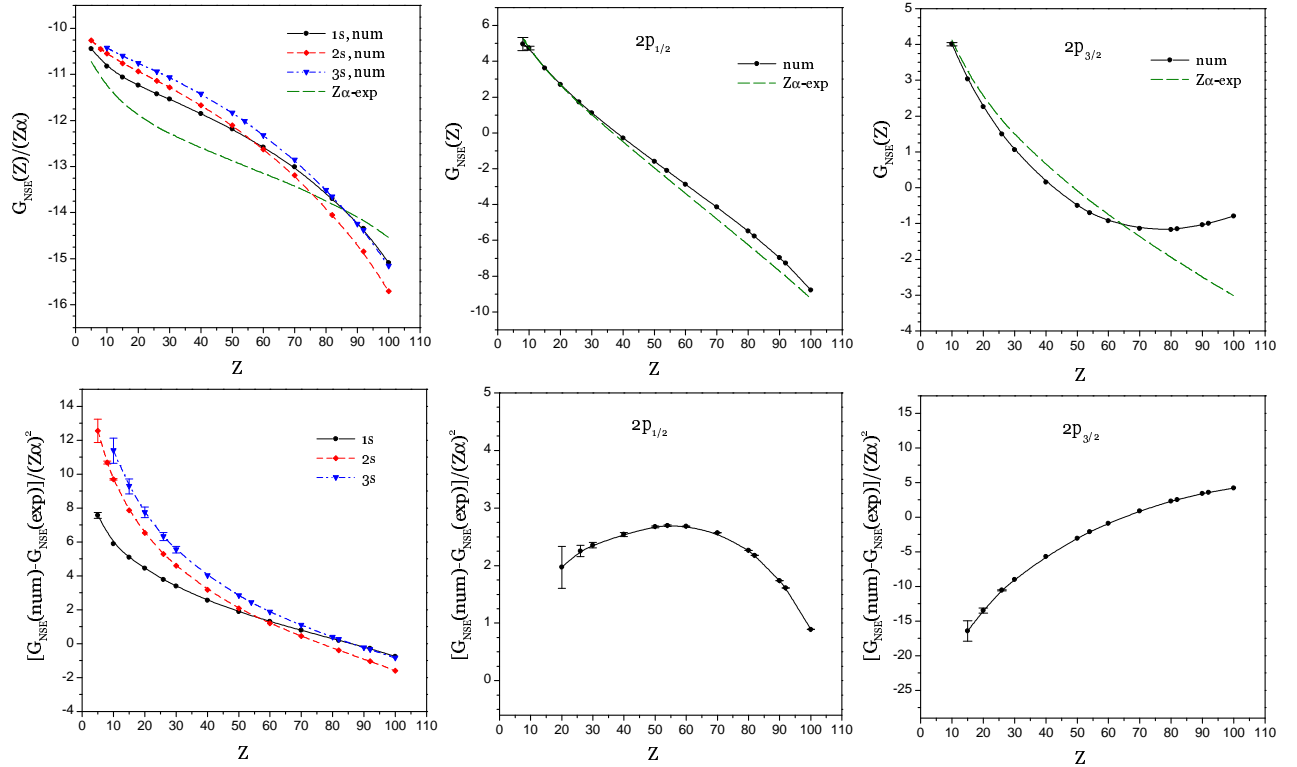


FIG. 1: (Color online) Nuclear-size self-energy correction, in terms of G_{NSE} defined by Eq. (9), as a function of the nuclear charge number Z . The upper graphs depict the ratio $G_{\text{NSE}}(Z)/(Z\alpha)$ for the ns states and the function $G_{\text{NSE}}(Z)$ for the np_j states, in comparison with the $Z\alpha$ -expansion results. The lower graphs show the difference between the all-order and $Z\alpha$ -expansion results for the function G_{NSE} divided by $(Z\alpha)^2$.

$r_b < r_a$ is allowed and it is assumed that $r_a > 0$. (The special case of $r_a = 0$ will be considered separately.) The

radial Dirac equation is (with $m = 1$)

$$G'(r) = -\frac{\kappa}{r} G(r) + (E - V(r) + 1) F(r), \quad (\text{A7})$$

$$F'(r) = \frac{\kappa}{r} F(r) - (E - V(r) - 1) G(r), \quad (\text{A8})$$

where $G(r) = rg(r)$ and $F(r) = rf(r)$ are the upper and

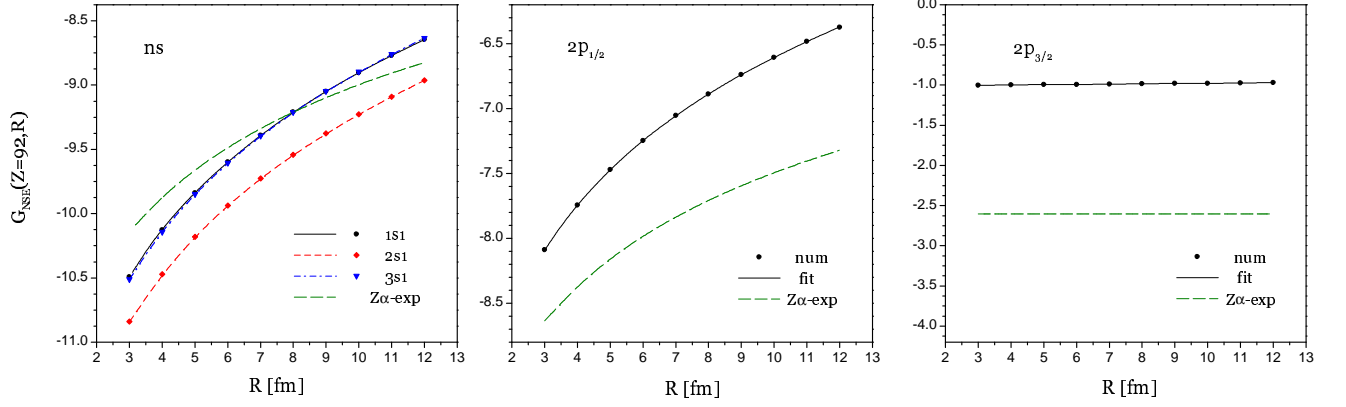


FIG. 2: (Color online) Nuclear-size self-energy correction, in terms of $G_{\text{NSE}}(Z\alpha, R)$ defined by Eq. (9), as a function of the rms nuclear charge radius R , for $Z = 92$.

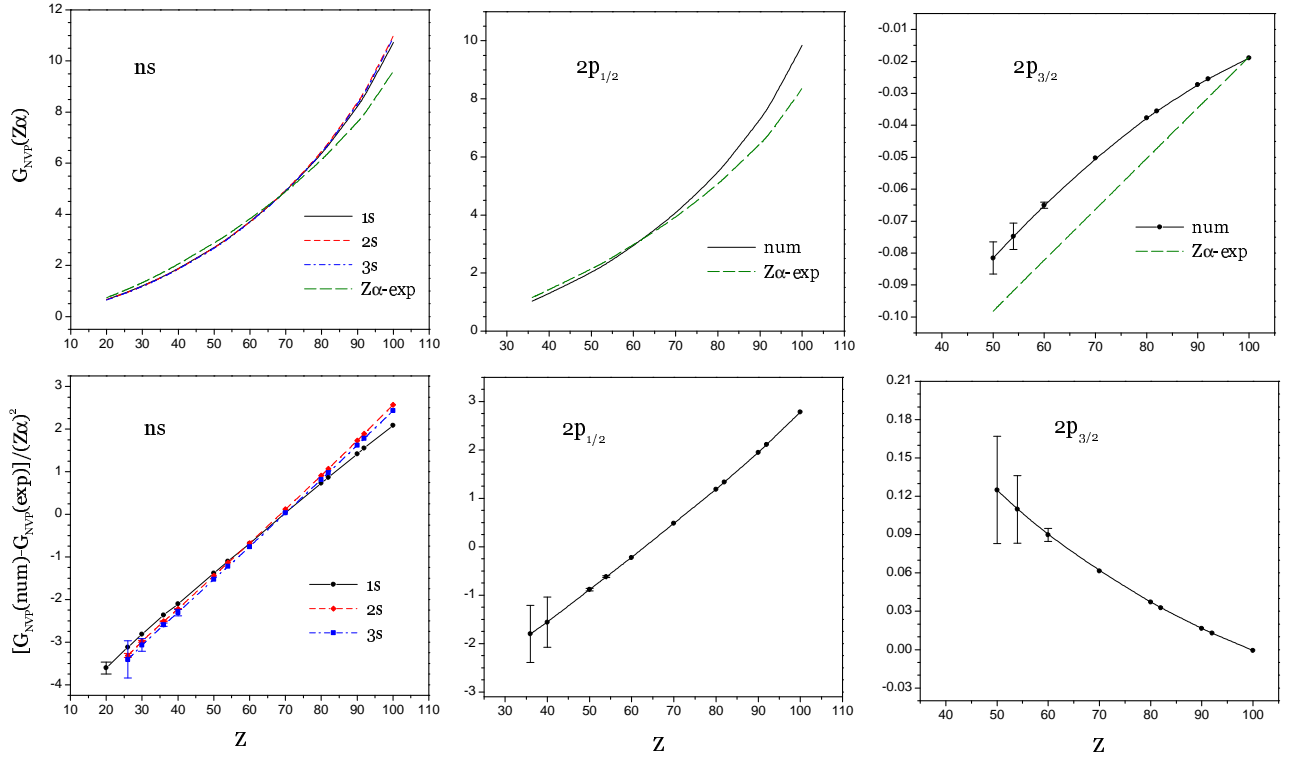


FIG. 3: (Color online) Nuclear-size vacuum-polarization correction, in terms of $G_{\text{NVP}}(Z\alpha, R)$ defined by Eq. (21), as a function of the nuclear charge number Z .

lower components of the radial Dirac solution. Introducing new variables $x = (r - r_a)/h$ and $h = r_b - r_a$, the equation is written as

$$(xh + r_a)G'_x + \kappa hG + UhF - (xh + r_a)hF = 0, \quad (\text{A9})$$

$$(xh + r_a)F'_x - \kappa hF - UhG - (xh + r_a)hG = 0, \quad (\text{A10})$$

where $U = r(V(r) - E)$. On the given interval, U is represented by a cubic polynomial of x , $U = \sum_{k=0}^3 u_k x^k$.

The solutions are represented as power series of the form

$$G(x) = \sum_{n=0}^{n_{\max}} a_n x^n, \quad F(x) = \sum_{n=0}^{n_{\max}} b_n x^n, \quad (\text{A11})$$

with the coefficients a_0 and b_0 determined by the boundary conditions $a_0 = G(r_a)$ and $b_0 = F(r_a)$. The coefficients a_n and b_n are determined by the recurrence rela-

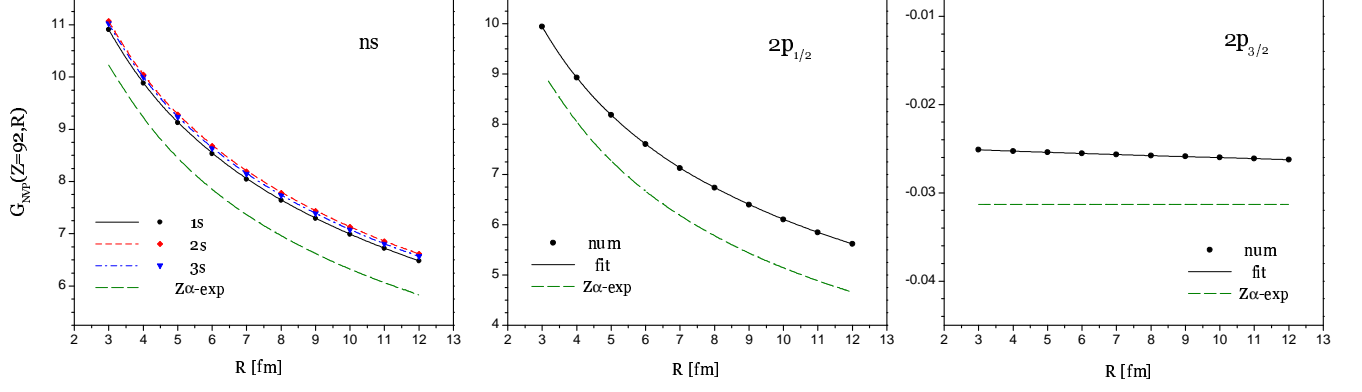


FIG. 4: (Color online) Nuclear-size vacuum-polarization correction, in terms of $G_{\text{NVP}}(Z\alpha, R)$ defined by Eq. (21), as a function of the rms nuclear charge radius R , for $Z = 92$.

TABLE IV: Coefficients of the $Z\alpha$ expansion of the NSE correction in Eq. (10).

Term	State	Value	Ref.
a_{01}	np_j	$8/9$	[4, 5]
a_{00}	$2p_{1/2}$	$0.808\,879\,967(1)$	[4, 5]
	$np_{3/2}$	$a_{00}(np_{1/2}) - 1$	[4, 5]
a_{10}	ns	$\pi(-23/4 + 4 \ln 2)$	[3, 22, 29]
	$np_{1/2}$	$\pi(379/432 - 16/3 \ln 2)$	[6]
	$np_{3/2}$	$\pi(559/432 - 4 \ln 2)$	[6]
a_{\log}	$ns, np_{1/2}$	$\pi^2/6 - 15/4$	[4, 22]
a_{22}	ns	$-2/3$	[23]
a_{21}	$np_{1/2}$	$-2(n^2 - 1)/n^2$	[23, 30]

tions (valid for $r_a \neq 0$)

$$a_n = -\frac{h}{nr_a}[(n-1+\kappa)a_{n-1} + (u_0 - r_a)b_{n-1} + (u_1 - h)b_{n-2} + u_2b_{n-3} + u_3b_{n-4}], \quad (\text{A12})$$

$$b_n = \frac{h}{nr_a}[(-n+1+\kappa)b_{n-1} + (u_0 + r_a)a_{n-1} + (u_1 + h)a_{n-2} + u_2a_{n-3} + u_3a_{n-4}]. \quad (\text{A13})$$

The solutions at the end point are given by the sum of the coefficients,

$$G(r_b) = \sum_{n=0}^{n_{\max}} a_n, \quad F(r_b) = \sum_{n=0}^{n_{\max}} b_n. \quad (\text{A14})$$

In the numerical evaluation, the recurrence relations are applied upwards until either the desired precision or the upper limit for n (typically, $n_{\max} = 30$) is reached. In the latter case, the interval is subdivided into two parts and the procedure is repeated until the desired accuracy is attained. This simple approach allows one to solve the equation with accuracy close to the machine precision.

Now, we consider the special case of $r_a = 0$. In this case, the solutions are represented by the power expansion of the form

of the form

$$G(x) = x^s \sum_{n=0}^{n_{\max}} a_n x^n, \quad F(x) = x^{s+t} \sum_{n=0}^{n_{\max}} b_n x^n, \quad (\text{A15})$$

where the parameters s and t are determined from the Dirac equation. For $\kappa < 0$, we have (for the regular potentials considered here) $s = |\kappa|$ and $t = 1$. The series start with

$$a_0 = 1, \quad b_0 = \frac{h + u_1}{1 + 2|\kappa|}. \quad (\text{A16})$$

The recursion relations take the form

$$na_n = (u_1 - h)b_{n-2} + u_2b_{n-3} + u_3b_{n-4}, \quad (\text{A17})$$

$$(2|\kappa| + n + 1)b_n = (h + u_1)a_n + u_2a_{n-1} + u_3a_{n-2}. \quad (\text{A18})$$

For $\kappa > 0$, one gets $s = \kappa + 1$ and $t = -1$. The series start with

$$a_0 = \frac{h - u_1}{1 + 2\kappa}, \quad b_0 = 1, \quad (\text{A19})$$

whereas the recursion relations are

$$(2\kappa + n + 1)a_n = (h - u_1)b_n - u_2b_{n-1} - u_3b_{n-2}, \quad (\text{A20})$$

$$nb_n = (u_1 + h)a_{n-2} + u_2a_{n-3} + u_3a_{n-4}. \quad (\text{A21})$$

Appendix B: One-potential Dirac Green function for a general potential

For the evaluation of the self-energy correction, the one-potential Dirac Green function $G^{(1)}$ is needed. Its radial part is defined as

$$G_{\kappa}^{(1)}(E, r_1, r_2) = \int_0^{\infty} dz z^2 V(z) G_{\kappa}^{(0)}(E, r_1, z) G_{\kappa}^{(0)}(E, z, r_2), \quad (\text{B1})$$

TABLE V: Different calculations of the Wichmann-Kroll vacuum-polarization correction [Eq. (19)] to the energy levels of H-like ions, in units $\Delta E/[(\alpha/\pi)(Z\alpha)^4/n^3]$.

Z	R [fm]	Model	$1s$	$2s$	$2p_{1/2}$	$2p_{3/2}$	Ref.
36	4.230	sphere	0.002 741 99(6)	0.002 833 98(3)	0.000 083 36(4)	0.000 027 95(4)	
		sphere	0.002 741 8	0.002 833 7	0.000 083 4	0.000 028 0	[25]
		shell	0.002 7	0.002 8	0.000 1	0.000 0	[15]
54	4.826	sphere	0.005 921 2(2)	0.006 423 4(2)	0.000 454 79(2)	0.000 114 18(5)	
		sphere	0.005 921 1	0.006 423 1	0.000 454 8	0.000 114 2	[25]
		shell	0.005 9	0.006 4	0.000 4	0.000 1	[15]
92	5.860	sphere	0.020 679 2(5)	0.027 252 0(8)	0.006 824 1(4)	0.000 749 49(6)	
		sphere	0.020 678 9	0.027 251 5	0.006 824 0	0.000 749 4	[25]
		shell	0.020 6	0.027 2	0.006 8	0.000 7	[15]

TABLE VI: Nuclear-size vacuum-polarization correction to the energy levels of H-like ions, in terms of the function $F_{\text{NVP}}(Z\alpha, R)$ defined by Eq. (21). Fermi model of the nuclear charge distribution is used. The nuclear charge rms radii used are listed in Table I. For a given Z , the upper line (“Ue”) corresponds to the Uehling part and the lower line (“WK”), to the Wichmann-Kroll part.

Z		$1s$	$2s$	$3s$	$2p_{1/2}$	$2p_{3/2}$
15	Ue	0.000 024 856	0.000 024 968	0.000 024 921	0.000 000 020	−0.000 000 016
20	Ue	0.000 047 62	0.000 048 21	0.000 048 12	0.000 000 102	−0.000 000 034
	WK	−0.000 006 4(2)	−0.000 006(1)	−0.000 006(3)		
26	Ue	0.000 089 44	0.000 091 72	0.000 091 60	0.000 000 402	−0.000 000 064
	WK	−0.000 012 58(1)	−0.000 012 9(1)	−0.000 013(1)		
30	Ue	0.000 131 907(2)	0.000 136 725(2)	0.000 136 601(2)	0.000 000 865	−0.000 000 092
	WK	−0.000 018 83(3)	−0.000 019 55(9)	−0.000 019 6(7)		
40	Ue	0.000 304 304(4)	0.000 326 352(4)	0.000 326 510(4)	0.000 004 205	−0.000 000 188
	WK	−0.000 043 43(4)	−0.000 046 5(1)	−0.000 046 6(9)	−0.000 000 9(1)	
50	Ue	0.000 674 503(2)	0.000 756 416(2)	0.000 758 099(2)	0.000 016 672	−0.000 000 342
	WK	−0.000 092 38(7)	−0.000 102 71(7)	−0.000 103 07(9)	−0.000 003 37(2)	−0.000 000 20(2)
60	Ue	0.001 410 95(1)	0.001 673 01(1)	0.001 680 03(1)	0.000 057 40	−0.000 000 546
	WK	−0.000 181 6(2)	−0.000 211 8(3)	−0.000 212 8(3)	−0.000 010 46(2)	−0.000 000 49(2)
70	Ue	0.003 100 32(1)	0.003 932 42(2)	0.003 956 23(2)	0.000 197 79	−0.000 000 872
	WK	−0.000 367 7(4)	−0.000 454 6(5)	−0.000 456 8(5)	−0.000 032 06(4)	−0.000 001 201(4)
82	Ue	0.007 710 07(4)	0.010 779 92(6)	0.010 863 65(6)	0.000 822 122(5)	−0.000 001 310
	WK	−0.000 821 5(7)	−0.001 106 2(9)	−0.001 111 4(9)	−0.000 114 34(9)	−0.000 003 021(4)
92	Ue	0.018 230 65	0.028 056 439(2)	0.028 275 306(4)	0.002 970 972	−0.000 001 923
	WK	−0.001 762 6(8)	−0.002 587(1)	−0.002 594(1)	−0.000 361 0(2)	−0.000 006 750(3)
100	Ue	0.036 429 910(6)	0.061 165 53(1)	0.061 549 11(1)	0.008 427 011(2)	−0.000 002 344
	WK	−0.003 259(2)	−0.005 184(4)	−0.005 183(4)	−0.000 915 4(6)	−0.000 012 100(6)

where $G^{(0)}$ is the free Dirac Green function. Substituting the representation (A1) for $G_{\kappa}^{(0)}$ into (B1) and introducing the integral functions

$$J_{\kappa}^{00}(r) = \int_0^r dz z^2 V(z) \varphi_{\kappa}^{0T}(z) \varphi_{\kappa}^0(z), \quad (\text{B2})$$

$$J_{\kappa}^{i0}(r) = \int_0^r dz z^2 V(z) \varphi_{\kappa}^{\infty T}(z) \varphi_{\kappa}^0(z), \quad (\text{B3})$$

$$J_{\kappa}^{ii}(r) = \int_r^{\infty} dz z^2 V(z) \varphi_{\kappa}^{\infty T}(z) \varphi_{\kappa}^{\infty}(z), \quad (\text{B4})$$

where $\varphi_{\kappa}^{(0)}$ ($\varphi_{\kappa}^{(\infty)}$) denote the regular (irregular) solutions of the free Dirac equation, we write the one-

potential Dirac Green function for $r_1 \leq r_2$ as

$$G_{\kappa}^{(1)}(E, r_1, r_2) = \Phi_{\kappa}^0(r_1) \varphi_{\kappa}^{\infty T}(r_2) + \varphi_{\kappa}^0(r_1) \Phi_{\kappa}^{\infty T}(r_2), \quad (\text{B5})$$

where

$$\Phi_{\kappa}^0(r) = \varphi_{\kappa}^{\infty}(r) J_{\kappa}^{00}(r) - \varphi_{\kappa}^0(r) J_{\kappa}^{i0}(r), \quad (\text{B6})$$

$$\Phi_{\kappa}^{\infty}(r) = \varphi_{\kappa}^{\infty}(r) J_{\kappa}^{i0}(r) + \varphi_{\kappa}^0(r) J_{\kappa}^{ii}(r). \quad (\text{B7})$$

For $r_1 > r_2$, the one-potential Green function is obtained by the symmetry condition,

$$G_{\kappa}^{(1)}(E, r_1, r_2) = G_{\kappa}^{(1)T}(E, r_2, r_1). \quad (\text{B8})$$

Analogously to the approach used for the full Dirac Green function, we store the functions φ_κ and Φ_κ on a radial grid $\{r_i\}_{i=1}^N$ and obtain the one-potential Green function by interpolation. The integral functions J_κ are evaluated by numerical integration with help of Gauss-Legendre quadratures. The integration interval $(0, \infty)$ is broken up at the position of the mesh points r_i , so that only one integral over $(0, \infty)$ needs to be evaluated

for a given value of E . Analogously to the case of the full Green function, all manipulations with the regular and irregular solutions are carried out after normalizing them according to Eqs. (A3) and (A4), in order to prevent numerical overflow and underflow. Similar method of computation of the one-potential Green function was used long ago by M. Gyulassy in his evaluation of the vacuum-polarization [31].

-
- [1] J. L. Friar, Z. Phys. A **292**, 1 (1979), [ibid. **303**, 84(E) (1981)].
 - [2] D. J. Hylton, Phys. Rev. A **32**, 1303 (1985).
 - [3] K. Pachucki, Phys. Rev. A **48**, 120 (1993).
 - [4] A. I. Milstein, O. P. Sushkov, and I. S. Terekhov, Phys. Rev. A **67**, 062111 (2003).
 - [5] U. D. Jentschura, J. Phys. A **36**, L229 (2003).
 - [6] A. I. Milstein, O. P. Sushkov, and I. S. Terekhov, Phys. Rev. A **69**, 022114 (2004).
 - [7] G. Soff and P. Mohr, Phys. Rev. A **38**, 5066 (1988).
 - [8] P. J. Mohr and G. Soff, Phys. Rev. Lett. **70**, 158 (1993).
 - [9] R. Pohl et al., Nature (London) **466**, 213 (2010).
 - [10] V. M. Shabaev, J. Phys. B **26**, 1103 (1993).
 - [11] F. Salvat, J. M. Fernández-Varea, and W. Williamson Jr., Comput. Phys. Commun. **90**, 151 (1995).
 - [12] V. M. Shabaev, I. I. Tupitsyn, V. A. Yerokhin, G. Plunien, and G. Soff, Phys. Rev. Lett. **93**, 130405 (2004).
 - [13] I. Angeli, At. Data Nucl. Data Tables **87**, 185 (2004).
 - [14] Y. S. Kozhedub, O. V. Andreev, V. M. Shabaev, I. I. Tupitsyn, C. Brandau, C. Kozhuharov, G. Plunien, and T. Stöhlker, Phys. Rev. A **77**, 032501 (2008).
 - [15] P. J. Mohr, G. Plunien, and G. Soff, Phys. Rep. **293**, 227 (1998).
 - [16] P. J. Mohr, Ann. Phys. (NY) **88**, 26 (1974).
 - [17] S. A. Blundell and N. J. Snyderman, Phys. Rev. A **44**, R1427 (1991).
 - [18] U. D. Jentschura, P. J. Mohr, and G. Soff, Phys. Rev. Lett. **82**, 53 (1999).
 - [19] K. T. Cheng, W. R. Johnson, and J. Sapirstein, Phys. Rev. A **47**, 1817 (1993).
 - [20] V. A. Yerokhin and V. M. Shabaev, Phys. Rev. A **60**, 800 (1999).
 - [21] V. A. Yerokhin, K. Pachucki, and V. M. Shabaev, Phys. Rev. A **72**, 042502 (2005).
 - [22] A. I. Milstein, O. P. Sushkov, and I. S. Terekhov, Phys. Rev. Lett. **89**, 283003 (2002).
 - [23] K. Pachucki, private communication, 2010.
 - [24] N. L. Manakov, A. A. Nekipelov, and A. G. Fainshtein, Zh. Eksp. Teor. Fiz. **95**, 1167 (1989), [Sov. Phys. JETP **68**, 673 (1989)].
 - [25] H. Persson, I. Lindgren, S. Salomonson, and P. Sunnergren, Phys. Rev. A **48**, 2772 (1993).
 - [26] J. Sapirstein and K. T. Cheng, Phys. Rev. A **68**, 042111 (2003).
 - [27] P. J. Mohr, B. N. Taylor, and D. B. Newell, Rev. Mod. Phys. **80**, 633 (2008).
 - [28] V. A. Yerokhin, A. N. Artemyev, V. M. Shabaev, and G. Plunien, Phys. Rev. A **72**, 052510 (2005).
 - [29] M. I. Eides and H. Grotch, Phys. Rev. A **56**, R2507 (1997).
 - [30] U. D. Jentschura and V. A. Yerokhin, Phys. Rev. A **81**, 012503 (2010).
 - [31] M. Gyulassy, Nucl. Phys. A **244**, 497 (1975).